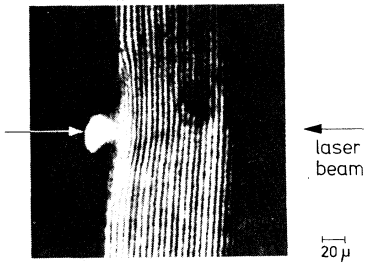

FIG. 5. Interferogram of Z discontinuity target. Arrow marks the position of the original discontinuity between aluminum and polyethene. $E = 23.6$ J. Time is same as in Fig. 2. Laser beam is incident from the right.

rise to large linear magnetic fields along the line of the discontinuity due to the density jump crossed with the axial temperature gradient. However, measurements on targets with a polyethene ($Z_{\text{eff}} = 3$) and aluminum ($Z = 13$) discontinuity showed no evidence of discontinuity fields, and additionally showed a reduction of an order of magnitude in thermoelectric fields. Additionally no evidence was obtained for a discontinuity from the interferometric data (Fig. 5), a result which is consistent with predictions of the MEDUSA code for the profile of the blowoff plasma for materials of different Z.

In conclusion, we have presented results with high spatial and temporal resolution of spatial profiles of magnetic fields in laser-produced plasmas. These fields are in good agreement with theoretical predictions and some shots show a possible reversed structure due to reversed density gradients in the off-axis density profile. Measurements of microballoon targets show the absence of sizable magnetic fields under conditions of uniform illumination. Contrary to suggestions in the literature, discontinuity targets failed to show enhanced magnetic fields or the predicted density discontinuity.

The authors would like to acknowledge the extremely helpful discussions with the National Research Laboratory Laser Plasma Interaction Group, in regard to measurement techniques, and the support of the Rutherford Laboratory Laser Division staff.

[a] Present address: Rutherford Laboratory, Chilton, Didcot, Oxon OX11 0QK, United Kingdom.

[1] J. A. Stamper *et al.*, Phys. Rev. Lett. 26, 1012 (1971).
[2] D. G. Colombant and N. K. Winsor, Phys. Rev. Lett. 38, 697 (1977).
[3] J. J. Thomson, C. E. Max, and K. Estabrook, Phys. Rev. Lett. 35, 633 (1975).
[4] D. A. Tidman, Phys. Rev. Lett. 32, 1179 (1974).
[5] A. Raven and P. T. Rumsby, Phys. Lett. 60A, 42 (1977).
[6] W. F. DiVergilio *et al.*, Phys. Rev. Lett. 38, 541 (1977).
[7] J. A. Stamper and B. H. Ripin, Phys. Rev. Lett. 34, 138 (1975); J. A. Stamper, E. A. McLean, and B. H. Ripin, Phys. Rev. Lett. 40, 1177 (1978).
[8] R. S. Adrain, E. G. Arthurs, and W. Sibbett, Opt. Commun. 15, 290 (1975).
[9] R. Illingworth, private communication.
[10] H. Azechi *et al.*, Phys. Rev. Lett. 39, 1144 (1977); R. Fedosejevs *et al.*, Phys. Rev. Lett. 39, 932 (1977).
[11] C. E. Max, W. M. Manheimer, and J. J. Thomas, Phys. Fluids 21, 128 (1978).
[12] E. Storm, private communication.

Drift Alfvén Waves in Tokamaks

K. T. Tsang, J. C. Whitson, J. D. Callen, P. J. Catto, and Julius Smith
Fusion Energy Division, Oak Ridge National Laboratory, Oak Ridge, Tennessee 37830
(Received 22 May 1978)

A new branch of solutions of the finite-beta drift-wave radial eigenmode equations has been found. The branch is heavily damped in the low-beta regime and identified with the shear Alfvén wave. This branch and the usual electrostatic branch are damped in a collisionless plasma. Including trapped electron effects introduces an instability which is potentially harmful to plasma confinement.

The recent interest in the possibility of explaining the anomalous electron heat transport in tokamaks as caused by magnetic field fluctuations associated with drift waves[1] has resulted in attempts[2,3] to improve earlier work by Catto *et al.*[4] for sheared magnetic fields. The equa-

tions used permit both unstable drift and unstable shear Alfvén waves[5] in the local approximation. Previously, retaining magnetic shear resulted in finite-beta modifications of the drift wave, where beta is the ratio of plasma pressure to magnetic pressure. In collisionless plasmas, this drift branch reduces to the stable collisionless drift wave of electrostatic theory[6,7] as $\beta \to 0$.

In this Letter we report the discovery of the collisionless shear Alfvén eigenmode in the presence of a sheared magnetic field. We find by numerical integration of the eigenmode equations that both the drift and shear Alfvén waves are stable in the collisionless slab limit considered. Consequently, both modes that can be unstable according to the local theory are always stable in a sheared magnetic field. However, if trapped electrons are included both the drift and shear Alfvén branches can be unstable. The trapped-electron drift mode[8] is unstable in the electrostatic limit and is found numerically to be gradually stabilized by finite-beta effects. This result agrees with previous analytic prediction.[9,10] On the other hand, the trapped-electron shear Alfvén mode is more unstable as beta increases and thus more harmful to the confinement of a high-beta tokamak.

For simplicity we adopt a slab plasma geometry with the inhomogeneity in the x direction. The magnetic field is assumed to be $\vec{B} = B(\hat{z} + x\hat{y}/L_s)$ where $\hat{y}$ and $\hat{z}$ are unit vectors in the y and z directions and L_s is the shear length. Such a model suffices to demonstrate the existence of radial eigenmodes even though it neglects the coupling of poloidal Fourier harmonics due to toroidal effects. We choose to locate the $k_\parallel = 0$ surface at $x = 0$, where $k_\parallel = kx/L_s$ denotes the parallel wavelength. For $m_e/m_i < \beta < 1$, we need introduce only the parallel component of the fluctuating vector potential $A_\parallel$ in addition to the fluctuating electrostatic potential φ. We seek solutions of the form $\varphi(x)\exp(-i\omega t + iky)$ and $A_\parallel(x)\exp(-i\omega t + iky)$. Using Ampere's law and the neutrality condition, we obtain the coupled equations for $\varphi(x)$ and $A_\parallel(x)$:

$$x\left(\frac{d^2}{dx^2} - k^2\right)A_\parallel = \alpha\left(\frac{d^2}{dx^2} - \kappa\right)\varphi, \tag{1}$$

$$\left(\frac{d^2}{dx^2} - \kappa\right)\varphi = (\lambda - \mu^2 x^2 + \sigma_e)\left(\varphi - \frac{\nu A_\parallel}{\alpha x}\right), \tag{2}$$

where

$$\kappa = \rho_i^{-2}(1 - \Gamma_0)/(\Gamma_0 - \Gamma_1),$$

$$\lambda = \rho_i^{-2}(\omega - \omega_*)/(\tau\omega + \omega_*)(\Gamma_0 - \Gamma_1),$$

$$\nu = \alpha\omega L_s/kc,$$

$$\alpha = c\beta_i(\tau\omega + \omega_*)(\Gamma_0 - \Gamma_1)L_s m_i/kT_e,$$

$$\beta_i = 4\pi NT_i/B^2, \quad \omega_* = kcT_e/eBL_n,$$

$$\Gamma_n = I_n(b)\exp(-b), \quad b = (k\rho_i)^2,$$

$$\rho_i^2 = m_i T_i c^2/(eB)^2, \quad \tau = T_e/T_i,$$

I_n is the modified Bessel function, N is density, and T is temperature. The $\mu^2 x^2$ term is the usual shear term due to the ion inertia and μ is defined by

$$\mu^2 = T_i\Gamma_0[m_i\rho_i^2(\Gamma_0 - \Gamma_1)]^{-1}(k/L_s\omega)^2.$$

For collisionless drift Alfvén waves, σ_e is given by

$$\sigma_e = \rho_i^{-2}\xi_e Z(\xi_e)(\omega - \omega_*) \times(\tau\omega + \omega_*)^{-1}(\Gamma_0 - \Gamma_1)^{-1}, \tag{3}$$

where $\xi_e = \omega/k_\parallel v_e = \omega L_s/xkv_e$, $v_e = (2T_e/m_e)^{1/2}$, and Z is the plasma dispersion function.

Equations (1) and (2) reduce back to the corresponding equations derived in Ref. 4 in the long-perpendicular-wavelength limit, i.e., $b \ll 1$. It is important to retain finite-ion-gyroradius effects, because for $\beta \to 0$ the collisionless drift wave was found to be less stable as b increases.[6,7]

Since we are looking for unstable modes with finite spatial extent in the x direction, one of the boundary conditions for φ and $A_\parallel$ is that they both vanish at large x. The symmetric property in x of Eqs. (1) and (2) requires the existence of two types of eigenmodes: even (in x) φ, odd (in x) $A_\parallel$, and vice versa. Thus the parity of φ and $A_\parallel$ is imposed as a boundary condition at $x = 0$. However, when we follow unstable modes to the stable region using Eqs. (1) and (2), no localized solution exists for real x. It is then necessary to detour the path of numerical integration in the complex x plane such that φ and $A_\parallel$ of the same branch of the mode fall off to zero at infinity. A simpler way to avoid this difficulty is to include the ion Z function in the perturbed ion density. In that case, Eq. (2) becomes

$$\left[\xi_i Z(\xi_i)\frac{d^2}{dx^2} - \kappa\right]\varphi = (\lambda + \sigma_e + m)\left(\varphi - \frac{\nu A_\parallel}{\alpha x}\right), \tag{4}$$

where

$$M=\Gamma_0[1+\xi_i Z(\xi_i)]/\rho_i^2(\Gamma_0-\Gamma_1),$$

$$\xi_i=\omega/k_\parallel v_i=\omega L_s/xkv_i,$$

and $v_i^2=2T_i/m_i$. With Eqs. (1) and (4) we can impose the boundary condition that both φ and $A_\parallel$ go to zero at sufficiently large x.

Our numerical procedure is an extension of the method used in the electrostatic problem.[6] In fact, the results reported in Ref. 6 were discovered when we attempted to check whether our finite-beta code could properly reproduce the electrostatic limit. In the finite-beta case, the code is checked against the following analytic dispersion relation,[4] derived from Eqs. (1) and (2) by assuming that $b=0$ and σ_e is independent of x, and demanding $\varphi'(x=0)=0$:

$$\mu\nu+i(1-4\lambda'\nu)^{1/2}+(\lambda'/\mu)=0, \tag{5}$$

where $\lambda'=\lambda+\sigma_e$. Our code employs a constant σ_e in Eq. (2) and reproduces eigenvalues in agreement with the prediction of Eq. (4) within 1% for beta up to 10%.

In the absence of magnetic shear, i.e., $k_\parallel$ = const, Eqs. (1) and (2) can be reduced to a dispersion relation of drift and shear Alfvén waves coupled by finite-ion-gyroradius effect. However, when magnetic shear is retained, the shear Alfvén waves have never been recovered. The difficulty is inherent to the local dispersion relation of the shear Alfvén wave: It is impossible to satisfy $\omega\sim k_\parallel v_A$ everywhere since $k_\parallel$ is a function of x while $v_A=B/(4\pi Nm_i)^{1/2}$ is essentially a constant. Because of this, one would expect the shear Alfvén wave in a sheared magnetic field to have a dispersion relation very different from that given by local theory.

Numerically solving Eqs. (1) and (4) with σ_e given by Eq. (3), we find two types of eigenmodes with different characteristics. The first type (the drift branch) is evolved from the electrostatic drift mode[6,7] gradually. Except for small b, this branch becomes more stable as beta increases. Another branch corresponds to the shear Alfvén mode and is heavily damped for small beta. As beta increases, the branch becomes less stable.

In Fig. 1, we plot the growth rates of the drift mode and shear Alfvén mode as functions of β_i for even φ and odd $A_\parallel$. Figure 2 shows plots for odd φ and even $A_\parallel$. The parameters are $\tau=1$ and $L_s/L_n=16$. The real part of ω for the drift mode decreases compared with ω_* as b increases. In contrast, the real frequency of the shear Alfvén mode stays around ω_*, almost independent of b. The mode frequency as a function of $k\rho_i$ for these two modes is plotted in Fig. 3 at a fixed β_i for even φ and odd $A_\parallel$. Similar conclusions hold for odd φ and even $A_\parallel$.

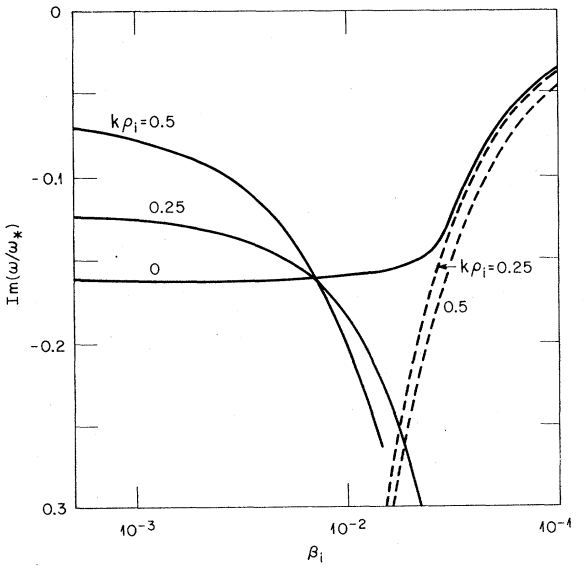

FIG. 1. Growth rates normalized by ω_* as functions of β_i for drift modes (solid lines) and shear Alfvén modes (broken lines) in a collisionless plasma with even φ, odd $A_\parallel$, $\tau=1$, and $L_s/L_n=16$.

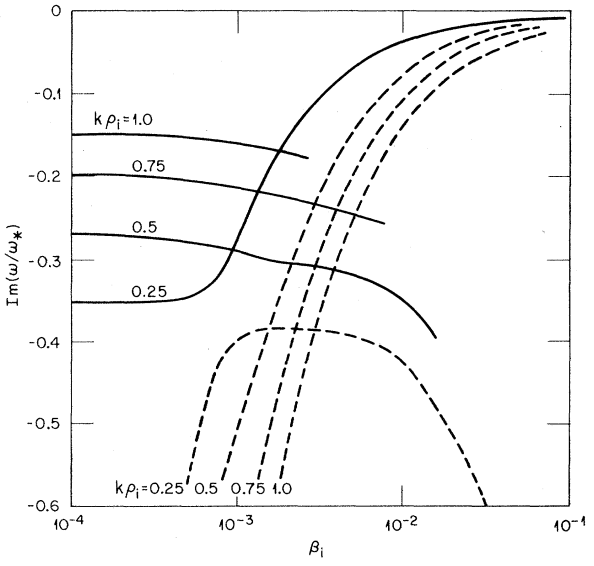

FIG. 2. Growth rates normalized by ω_* as functions of β_i for drift modes (solid lines) and shear Alfvén modes (broken lines) in a collisionless plasma with odd φ, even $A_\parallel$, $\tau=1$, and $L_s/L_n=16$.

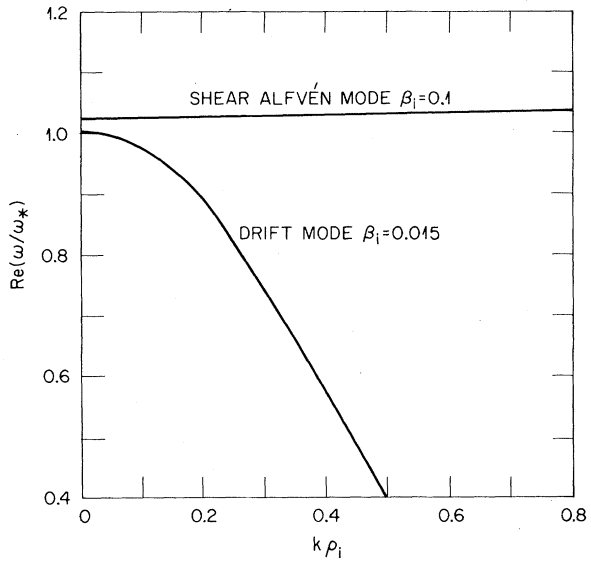

FIG. 3. Real part of ω as a function of $k\rho_i$ for the drift mode and the shear Alfvén mode.

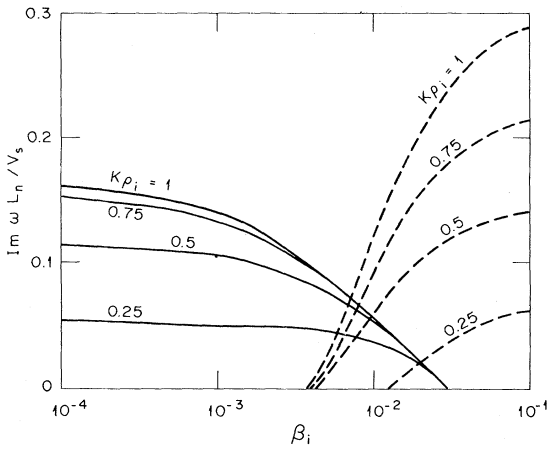

FIG. 4. Growth rates normalized by v_s/L_n as functions of β_i for the trapped-electron drift wave (solid lines) and the trapped-electron shear Alfvén wave (broken lines) with even φ, odd $A_\parallel$, $\tau=1$, $L_s/L_n=16$, $q=2$, $\nu_*=10^{-2}$, $\eta_e=1$, and $\epsilon=\epsilon_n=0.2$, where $v_s=(T_e/m_i)^{1/2}$ is the ion sound speed. Note that for current values of $\beta\sim1\%$, the shear Alfvén branch may dominate the drift branch.

In Fig. 2, we omit the investigation of odd-φ, even-$A_\parallel$ modes with $k\rho_i\approx 0$ because such modes are not localized; they can only exist by coupling to outside MHD (magnetohydrodynamic) solutions. This is beyond the scope of this Letter.

The $k\rho_i\approx0$ case for even φ and odd $A_\parallel$ is of particular interest because it is the only one for which analytic solutions of Eqs. (1) and (2) are available.[2-4] All of these analytic results predict that finite-beta effects will further stabilize the mode. Numerically, we found that the stabilizing effect is so small that it can hardly be observed from Fig. 1. When $\beta\gtrsim L_n/L_s$, the mode is far less stable than would be predicted by the analytic results. A plot of the eigenfunction shows that at this high beta the radial eigenmode is rapidly decaying spatially for $x>x_+\sim\mu^{-1/2}$, which is the turning point distance in the electrostatic equation. This spatial decay occurs because high beta ($>L_n/L_s$) results in a barrier, thereby reducing the amount of wave energy leaked to the region where ion Landau damping occurs, thus making the mode less stable. Similar conclusions can be drawn from the WKB form of solution of Eqs. (1) and (2). For $k\rho_i>0$, the drift mode is further stabilized by finite-beta effects, as expected.[2-4]

Because the real part of ω for the drift mode and the shear Alfvén mode with $k\rho_i=0$ is close to ω_*, both modes seem to be degenerate. We cannot find a shear Alfvén mode with $k\rho_i=0$ which is heavily damped at low beta. This conclusion is backed up by a careful search of the relevant region of ω space using the Cauchy integral method.

When the trapped-electron response is included (as in Ref. 9, except that the Landau resonance of the circulating electrons is ignored since it is usually small compared with the trapped-electron response), we find that the electrostatic trapped-electron mode is gradually stabilized by finite-beta effects as beta increases from zero. This is illustrated by the solid lines in Fig. 4 for a typical set of parameters: $\partial\ln T_e/\partial\ln N=1$, $L_n/R=r/R=0.2$, $q=2$, $\nu_{*_e}=10^{-2}$, and $L_s/L_n=16$, where ν_{*_e} is the collisionality of the electrons, defined as the ratio of the mean effective collision frequency to the mean bounce frequency of trapped electrons. For this set of parameters, the trapped-electron drift mode is completely stabilized for $\beta_i\gtrsim3\%$, and the shear Alfvén mode is stable for $\beta_i\gtrsim0.4\%$. Around $\beta_i=1\%$, the typical value of beta for present experiments, the growth rate of the shear Alfvén mode is already larger than that of the drift mode and continues to increase with beta. These results on the finite-beta, trapped-electron, drift Alfvén instabilities are by no means final because of the crudeness of our model equations. Even though a similar model is used in the careful analysis by Tang *et al.*,[9] there is singularity in these eigenmode equations. A more detailed and careful study is

in progress.

In conclusion, we have demonstrated numerically the existence of shear Alfvén waves in tokamak geometry. Both the drift wave and the shear Alfvén wave are stable in a collisionless plasma. When trapped electrons are included, both waves can be unstable. However, their behaviors with beta are different. While the drift mode is stabilized by effects of beta, the shear Alfvén mode is destabilized. Of course, when the poloidal beta approaches $1/\epsilon$, the simple concentric, circular flux-surface model used to calculate the trapped-electron response and the slab model underlying Eqs. (1) to (4) are no longer valid. For these reasons, the high-beta ends of the curves in Figs. 1, 2, and 4 are not very accurate but should still represent the beta dependence of the usual drift and the shear Alfvén branch in a tokamak with $\beta \lesssim 5\%$.

This research was sponsored by the Office of Fusion Energy (ETM), U. S. Department of Energy under Contract No. W-7405-eng-26 with the Union Carbide Corporation.

[1]J. D. Callen, Phys. Rev. Lett. 39, 1540 (1977).
[2]L. Chen, J. Hsu, P. K. Kaw, and P. H. Rutherford, Princeton Plasma Physics Laboratory Report No. 1376, 1977 (unpublished).
[3]S. M. Mahajan and D. W. Ross, University of Texas Report No. FRCR 157, 1977 (unpublished).
[4]P. J. Catto, A. M. El Nadi, C. S. Liu, and M. N. Rosenbluth, Nucl. Fusion 14, 405 (1974).
[5]A. B. Mikhailovskii and L. I. Rudakov, Zh. Eksp. Teor. Fiz. 44, 912 (1963) [Sov. Phys. JETP 17, 621 (1963)].
[6]K. T. Tsang, P. J. Catto, J. C. Whitson, and Julius Smith, Phys. Rev. Lett. 40, 327 (1978).
[7]D. W. Ross and S. M. Mahajan, Phys. Rev. Lett. 40, 324 (1978).
[8]B. B. Kadomtsev and O. P. Pogutse, Dokl. Akad. Nauk SSSR 186, 553 (1969) [Sov. Phys. Dokl. 14, 470 (1969)].
[9]W. M. Tang, C. S. Liu, M. N. Rosenbluth, P. J. Catto, and J. D. Callen, Nucl. Fusion 16, 191 (1976).
[10]A. B. Mikhailovskii, Dokl. Akad. Nauk SSSR 228, 1317 (1976) [Sov. Phys. Dokl. 21, 339 (1976)].

Incipient Superfluidity in Liquid ^{3}He above the Superfluid Transition Temperature

D. N. Paulson and J. C. Wheatley
Department of Physics, University of California, San Diego, La Jolla, California 92037
(Received 5 May 1978)

The large zero-sound attenuation just below the transition temperature T_c to a superfluid state in liquid ^{3}He is anticipated above the transition by an excess attenuation over that for a normal Fermi liquid. The excess is greatest at T_c but can be readily discerned at temperatures several percent above T_c. The excess is largest near melting pressure and exists adjacent to both ^{3}He-A and ^{3}He-B.

The attenuation of zero sound[1-3] in a normal Fermi liquid is frequency independent and proportional to T^2. We have discovered that in liquid ^{3}He at temperatures above the transition temperature T_c the zero-sound attenuation rises above the extrapolated value for normal zero-sound attenuation. The excess attenuation is very significant, readily measurable, and can be discerned at temperatures as much as 10% above T_c. That such an effect might exist for zero sound was pointed out some time ago by Paulson, Johnson, and Wheatley.[4] A small effect above T_c was observed in static magnetization by Paulson, Kojima, and Wheatley[5] and in viscosity coefficient by Parpia, Sandiford, Berthold, and Reppy,[6] the measurable effects extending above T_c by only a tenth of a percent of T_c. It is possible that the excess zero-sound attenuation reflects the fluctuation superfluidity in fermion systems first discussed by Thouless[7] (equilibrium properties) and by Emery[8] (transport properties). In particular, Emery[8,9] has stressed the possible importance of fluctuation superfluidity to an understanding of the properties of liquid ^{3}He, while fluctuations in *superconductors* have proven to be of great interest.[10] Although there does not yet exist a theory of the excess attenuation which we describe here, we hope that this work will stimulate a theoretical interpretation so that, in analogy to superconductivity, a deeper understanding of the superfluid state will result.

Our measurements were made in a nuclear

